RSC Advances

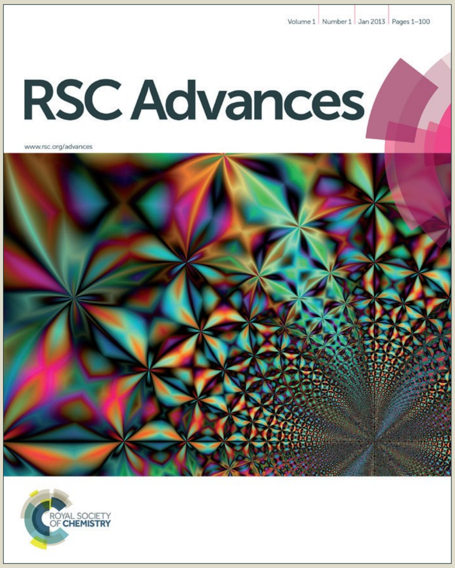

Study the Supercapacitive behavior of polyaniline/Nano structural manganese dioxide composite using Fast Fourier transforms continuous cyclic voltammetry.

Javad Shabani shayeh, Parviz Norouzi*, Mohammad Reza GanjAli.

Institute of Electrochemistry, University of Tehran, Tehran, Iran

* Corresponding author. Tel.: +98 21 61112788; fax: +98 21 66495291. E-mail address: norouzi@khayam.ut.ac.ir (P. Norouzi).

Abstract

In this work supercapacitive behavior of electrochemically synthesized polyaniline/ Nano structure manganese dioxide composite (PANI/NsMnO$_2$) on Glassy Carbon electrode (GCE) was studied. NsMnO$_2$ was synthesized by ultrasound method. PANI/NsMnO$_2$ was synthesized by cyclic voltammetry in 1 M H_2SO_4 solution contained aniline monomer (0.03 M), NsMnO$_2$ (0.2% wt) and (5 mM) sodium dodecyl sulfate (SDS). The average size of NsMnO$_2$ that distributed unique in composite was 60 nm. Cyclic voltammetry (CV), galvanostatic charge–discharge (CD), electrochemical Impedance spectroscopy (EIS) and fast Fourier transform continues cyclic voltammetry (FFTCCV) methods were used for the study of supercapacitive properties of composite electrode. For morphology and structural characterizations of composite electrode scanning electron microscopic (SEM) and Fast Fourier transform Infrared spectroscopy (FTIR) were used. Specific capacity of PANI and PANI/NsMnO$_2$ using Cylicvoltametry were calculated 190 and 507 Fg^{-1} respectively. Stability of two electrodes were measured and compared with together FFTCCV technique. Presence of NsMnO$_2$ caused increasing the stability of electrodes from 30% for PANI to 90% for PANI/NsMnO$_2$ electrode. Furthermore by using FFTCCV technique changes in electrochemical behavior of PANI/NsMnO$_2$ composite electrode in overtime were scrutinized.

KEYWORDS: Supercapacitor, Polyaniline, Nano structural MnO$_2$, Fast Fourier Transform cyclic voltammetry, stability of electrode.

1 Introduction

Nowadays electrochemical capacitors (ECs) attract public attention to themselves for using in energy storage devises. based on charge storage mechanism ECs are divided to two parts.[1,2] The First is electric double layer capacitor (EDLC) that capacitance in them arises from charge separation and the second pseudo capacitances that capacitance is due to faradic reactions.[3,4] Also ECs classified in three groups based on active materials that are Active carbon, conductive polymers (CP) and metal oxides.[5,6]

CPs such as polyaniline (PANI), poly pyrrol (PPY), poly thiophen (PTP) and their derivatives are attractive material to use as supercapacitors.[7] PANI is most considered conductive polymer because of low cost, high conductivity, And the ease of synthesis than other conductive polymers.[8] Low cycle ability is the main problem that impeded the application of PANI in industry.[9] One of the reasons for poor cycle ability of polyaniline is degradation of polymer film during doping and undoping of counter ions. During cycles, the volume of polymer changes and some part of polymer chain solvated in water.[10,11] One of the methods for enhancement the stability of PANI is to make composite with some Nano materials like carbon Nano tube (CNT),[12] metal oxide[13] and other material.[14-15] Metal oxides are good candidate for coupling with CPs because their pseudocapacitive behaviors collaborated by capacitive performance of CPs. Some metal oxides like as RuO_2 have good pseudocapacitive behavior but because the toxicity and high cost, utilization of this material were neglected.[16] On the other hand metal oxides that have low cost and were environmentally friendly have got more attentions. MnO_2 is one of these materials that has above properties and synthesized by several methods.[17] Furthermore the capacitance of MnO_2 electrode is so high and for powder electrode is about 150-300 F/g.[18] Although thin film of MnO_2 electrode has more Capacitance, but they would suffer from poor energy density values. Also MnO_2 has high resistivity and equivalent series resistance (ESR) and for this problem MnO_2 combined with other active materials.[19] It has already been shown that the nanostructure of the MnO_2 can affects on charge–discharge properties of the pseudo capacitors, particularly at large current densities, having large specific surface area and enlarges the contact area between active and conducting are some Goals for chose the synthesis procedure of MnO_2. Various nano Structural composite electrodes of MnO_2 were synthesized via different methods.[20,21]

As mentioned, separately using of these materials is limited by their intrinsic structural shortcoming. Therefore making composite electrode is a good route for maximizing electrochemical effectiveness of metal oxides And CPs. pseudocapacitive performance of MnO_2 and high doping/undoping properties of conductive polymers are the other advantages of making composite. The best matrix for MnO_2 and CPs composites must be have high number of porosity, to have more amount of metal oxides and moreover high amount of sites for pseudo capacity behavior for CP. In this paper we synthesized PANI and PANI/NsMnO_2 composite electrodes electrochemically using cyclic voltammetry method and then rinse the electrode with double distilled water and after that put the electrode in 1M H_2SO_4 solution for electrochemical measurements. We used CV, CD, EIS and FFTCCV methods for fully comparing of PANI and PANI/NsMnO_2 electrodes together. For material characterizations electrode removed from cell dried in free air and used for SEM and FTIR studies.

Our attention in this study is to synthesis a composite electrode by PANI and NsMnO_2 with high amount porosity to reach to high performance for supercapacitors such as higher specific capacitance and more lifetimes during numerous cycles.

2 Experimental

2.1 Chemicals

All the chemical materials used in this work were Merck products of analytical grade and were used without further purification. Double distilled water was used throughout. Aniline was doubly distilled and the resulting colorless liquid was kept in the dark at 5°C. $NsMnO_2$ was synthesized by ultrasound method as described in the literature.[22]

A mixture of $MnSO_4$ (0.25 M) and $KBrO_3$ (0.5 M) solution was sonicated for 4h at 45°C. The obtained precipitates were washed several times with distilled water followed by ethanol to remove impurities, and then dried in vacuum at 110°C for 5h. The dried powder was put into muffle and heated at 300°C for additional 3h. These powders were acidified with 2 M H_2SO_4 at 90°C for 2h. Finally, the product was washed with distilled water and vacuum dried.

2.2 Synthesis of PANI and PANI/$NsMnO_2$ composite electrodes

PANI/$NsMnO_2$ composite was synthesized electrochemically by cyclic voltammetry in 1 M H_2SO_4 solution that contained aniline monomer (0.03 M), $NsMnO_2$ (0.2% wt) and sodium dodecyl sulfate (0.005 M) which were dispersed in the solution by sonication. PANI electrode was synthesized in same solution without $NsMnO_2$ and SDS. Polymerizations for both electrodes conducted by 10 cycles at the sweep rate of 50 mV s^{-1} in the potential window between -0.2 to 1.2 V. The mass of PANI films was approximated assuming a current efficiency for the electro polymerization process of 100% using Faraday's law of electrolysis.[23]

2.3 Materials characterization and electrochemical evaluation

Electrochemical experiments were carried out by an Autolab General purpose System PGSTAT 30 (Eco-chime, Netherlands). A conventional three electrode cell with a glassy carbon electrode with the area of 0.03 cm^2 as working electrode, Platinum wire and an Ag/AgCl reference electrode (Argental, 3 M KCl) were used as as counter and reference electrode, respectively. The EIS experiments were conducted in the frequency range between 100 kHz and 15 mHz with perturbation amplitude of 5 mV.

Morphological investigations of the polymeric films were carried out by using SEM (Philips XL 30). The Fourier transform infrared (FTIR) spectra were recorded on Nicolet 6700 with the sweeping range of 500–4500 cm^{-1} at a 4 cm^{-1} resolution with KBr as compressed slices.

2.4 FFTCCV technique

The FFT experimental data collection was performed with the help of the following equipment; a setup of a computer, equipped with a data-acquisition board (PCL-818HG, Advantech. Co.) And a custom-made potentiostat described in our previous works. A computer program that was developed in Delphi6® environment that used for data acquisition and data processing. The signal Calculation in this method is established based on the integration of net current changes over the scanned potential range. It must be noted that in this case, the current changes at the voltammograms can be caused by various processes, which take place at the electrode surface. In detail, a CV of the electrode was firstly recorded. Then, the existing high frequency noises were indicated by applying FFT on the collected data. With the help of this information, the cutoff frequency of the analog filter was set at a certain value where the noises were removed from the CV.[24-28]

3 Results and discussion

3.1 Characterizations

Fig.1 Shows the SEM graphs of PANI/NsMnO$_2$ electrode. As can be seen NsMnO$_2$ particles adhere on the surface of polyaniline filaments. These particles can connect polyaniline filaments together and improve their stability. The procedure is flowed by wrapping the PANI filament on the surface of nano particles or nano particle have been dispersed in the polymer matrix.[29,30] The average size of NsMnO$_2$ are 60 nm and this particles distributed in polymer matrix. It can be seen that the porosity of polymer film remained, however the pseudobehavior of the polymer can storage charges by doping-undoping process.

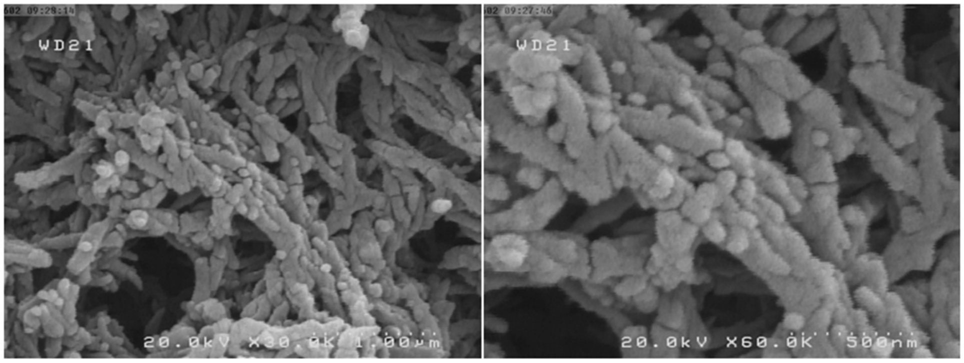

Fig.1. SEM graphs of PANI/NsMnO$_2$

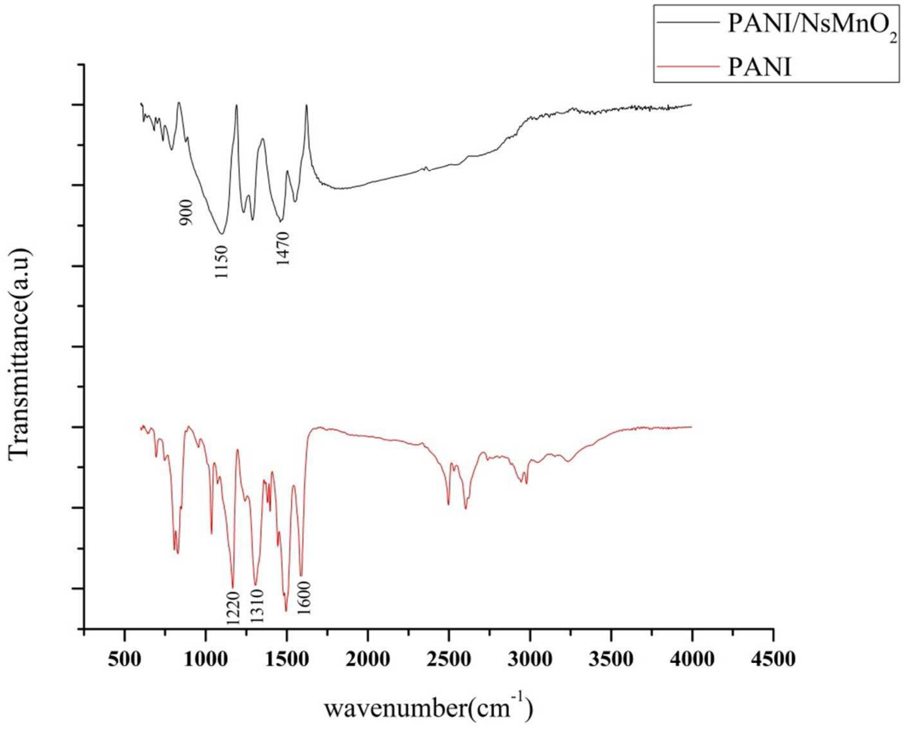

Fig. 2 . FTIR spectra of PANI and PANI/NsMnO$_2$.

The structure and component of PANI/NsMnO$_2$ composite elucidated by FTIR technique. Fig. 2. Presents the FTIR spectra of PANI and PANI/NsMnO$_2$. The adsorption peaks reveal the presence of both polyaniline and NsMnO$_2$, and can be identified as follow.[31-32]

The characteristic absorption bands of PANI appears at 1310 and 1600 cm^{-1}, corresponding to the stretching mode of C-N and C=N bands, reveal the presence of leucoemeraldine and permigraniline components.[33] CH$_2$ bending vibrations (1470, 900 cm^{-1}), C-N symmetric stretching vibration (1150 cm^{-1}) and 1167 cm^{-1} are related to the polyaniline conductivity and a degree delocalization of electrons. The regions from 500to 800 cm^{-1} can be assigned to stretching vibrations of Mn-O. Bands around 3400 and 1630 cm^{1} are observed for $NsMnO_2$ and $PANIMnO_2$product, due to the presence of interlayer or surface water.[34]

FTIR spectrum of the PANI-MnO_2 nano composite exhibits characteristic bands of PANI as well as of manganese oxide, which confirms the presence of both components in the nano composite.

3.2 Electrochemical measurement

Cyclic voltammetry examinations of fabricated electrodes were performed in potential range of 0.2 to 0.8 /V. The CV curves of two electrodes at the scan rate of 25 mV s^{-1} are shown in Fig.2a. As can be seen in all CV curves a pair redox peaks that related to the transition from emeraldine to pernigraniline form of PANI appear. Specific capacitance of electrodes calculated from CV curves according to following equation:

$$C = \frac{I}{mv} \qquad (1)$$

Where I is the current, m is the mass of reactive material and ν is the potential scan rate.

As can be seen the capacitance of composite electrode is almost three times more that that of the PANI one. The rectangular shape of PANI/$NsMnO_2$ shows that this composite has good electrochemical behavior as supercapacitive materials. The specific capacitance of PANI and PANI/$NsMnO_2$ were calculated 190 and 507 F/g respectively. Fig. 3b) presents the CVs of PANI/$NsMnO_2$ at various scan rates from 2 to 150 mV s^{-1}. symmetrical shape the electrode indicate high intrinsic electrical conductivity of composite film and good kinetic reversibility, which are important factors for supercapacitors. The deviation from rectangularity of CVs becomes obvious as scan rate increases. This phenomenon can be attributed to the electrolyte and film resistance, and this distortion is depending on scan rate.

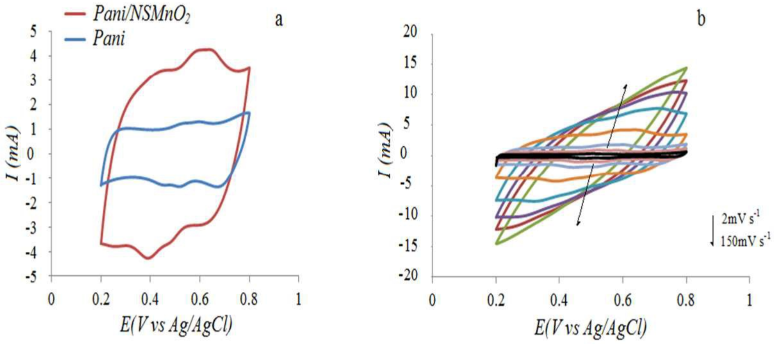

Fig. 3. a) CV curves PANI and PANI/NsMnO$_2$ electrode at the scan rate of 25 mV s^{-1} in 1M H_2SO_4 solution, b) CVs of PANI/NsMnO$_2$ electrode at various scan rate in 1M H_2SO_4 solution.

Fig. 4. Presents specific capacitance of PANI/NsMnO$_2$ electrode at different scan rates. as can be seen the Specific capacitance of electrodes decreased by increasing scan rates because in fast sweep rates just outer porosity are use and deeper those are not accessible for doping / undoing process.[35]

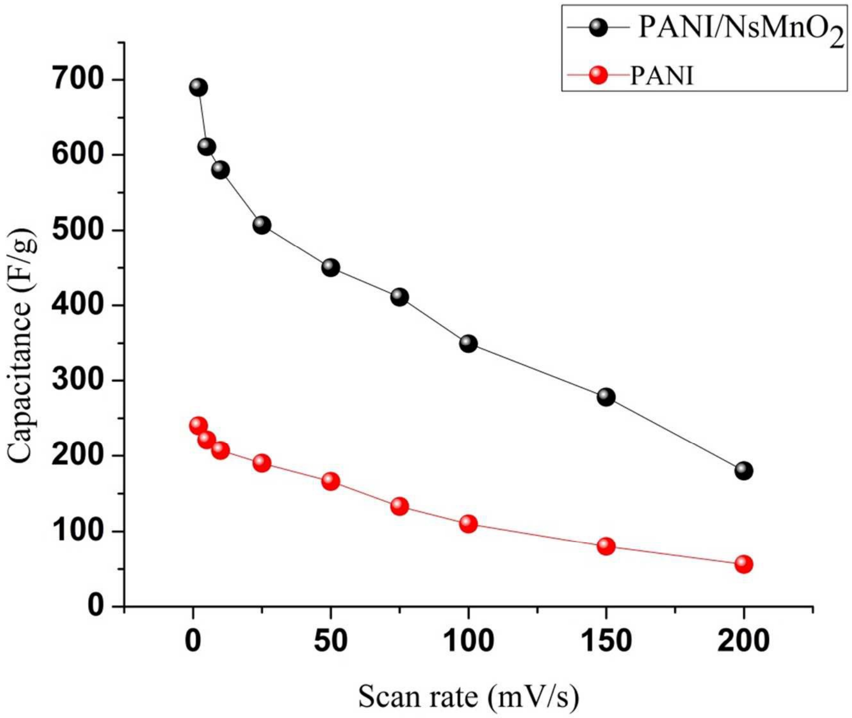

Fig. 4. specific capacitance of the PANI and PANI/NsMnO$_2$ electrodes as a function of scan rates.

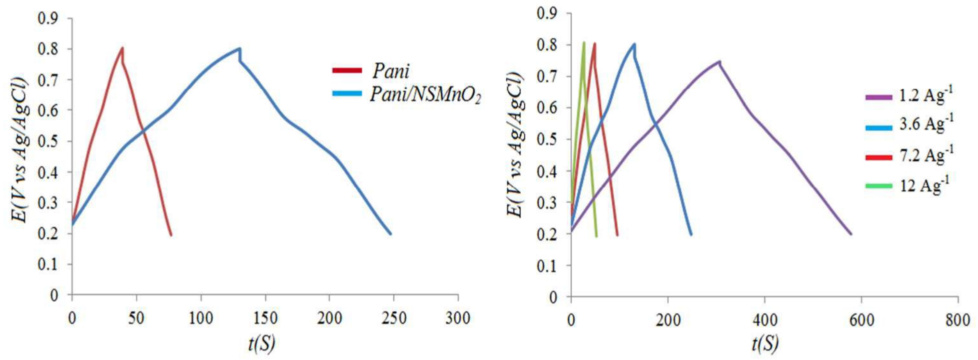

Fig. 5. a) CDs of PANI and PANI/NsMnO$_2$ electrodes in 1M H_2SO_4 at current of 1.2A/g, b) CDs of PANI/NsMnO$_2$ electrode in 1M H_2SO_4 at various currents.

One of The most direct approaches to evaluate the applicability of supercapacitor materials is the CD study. Fig. 5a shows the typical CD curves of the PANI and PANI/NsMnO$_2$ electrodes. From the figure, it can be seen that PANI/NsMnO$_2$ electrode has more capacitive characteristic than PANI electrode. This is consistent with the results of CV curves. Improvement the capability of charge storage by increasing the porosity of polymer film and pseudobehavior of NsMnO$_2$ caused to this synergistic effect of composite. Furthermore as can be seen the magnitude of equivalent series resistance (ESR) of composite electrode is smaller than PANI that depicted higher conductivity of composite film than PANI electrode. Fig. 5b presents CD curves of PANI/NsMnO$_2$ electrode at various constant currents. As can be seen by increasing the magnitude of current densities, symmetrical shape of curves preserved. But ESR magnitude in the curves increased. The symmetrical shape of CD curves shows that PANI/NsMnO$_2$ has suitable charge storage performance at various current densities. Here, SC was measured according to the CD curves, using Eq. (2).

$$\mathrm{SC} = \frac{\mathrm{I}}{-(\frac{\Delta \mathrm{E}}{\Delta \mathrm{t}})\,\mathrm{m}} \qquad (2)$$

In this equation *I* is the applied current; $-\frac{\Delta E}{\Delta t}$ is the slope of the discharge curve after the voltage drop at the beginning of each discharge (ESR); and m was the mass Reactive material. The most SC for composite electrode was obtained when the current density for charge/discharge process was 1.2 A/g.

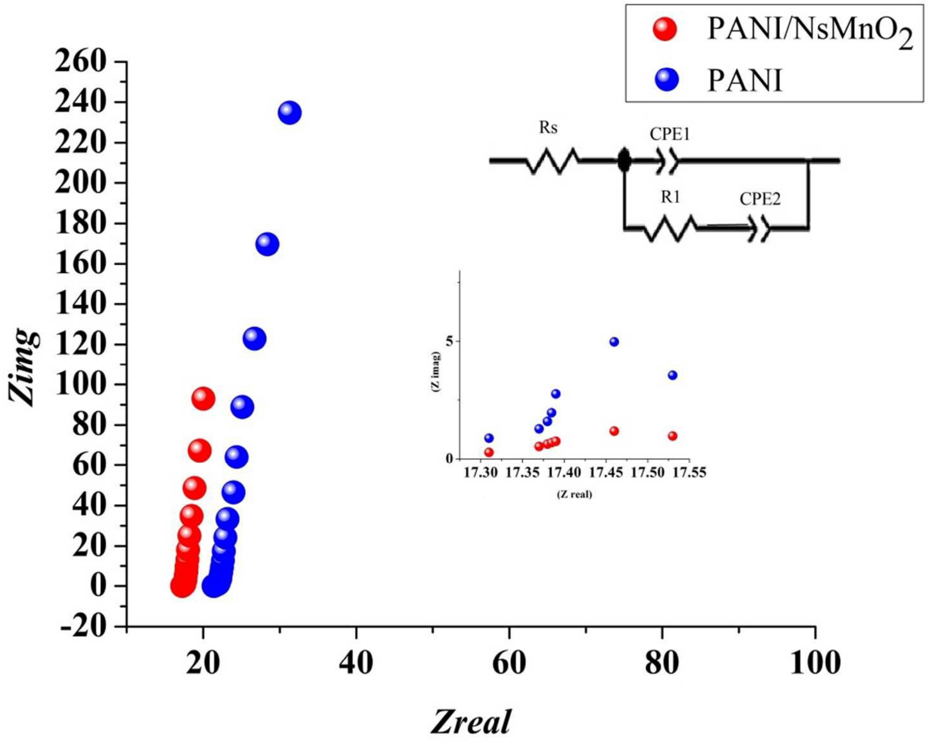

Fig. 6. Nyquist plots of the PANI and PANI/NsMnO$_2$ electrodes in1M H$_2$SO$_4$ solution.

The electrochemical impedance study was tested for two electrodes with the goal of investigating the electrochemical behavior of electrodes/electrolyte interface in detail. As can be seen from Fig. 6. Nyquist diagrams consist of a semicircle in the high frequency region followed by a nearly vertical straight line in the low frequency. The equivalent circuit compatible with the Nyquist diagram was depicted in Fig. 6. To obtain a satisfactory impedance simulation, it is necessary to replace the capacitor *C* with a constant phase element (*CPE*) in the equivalent circuit. The most widely accepted explanation for the presence of *CPE* behavior and depressed semicircles on solid electrodes is microscopic roughness, causing an inhomogeneous distribution in the solution resistance as well as in the double-layer capacitance.[36-38] The capacitance (C_{lf}) of each Electrode was determined from the Eq. (3):

$$C_{lf} = \frac{1}{2\pi f Z''} \qquad (3)$$

In which f is the frequency, and Z'' is the imaginary component of impedance. The SC of PANI and PANI/NsMnO$_2$ were calculated 177 and 451F/g, respectively. It can be seen that PANI/NsMnO$_2$ electrode had more capacitance than PANI electrode. These results also confirmed the data that obtained by CV and CD methods.

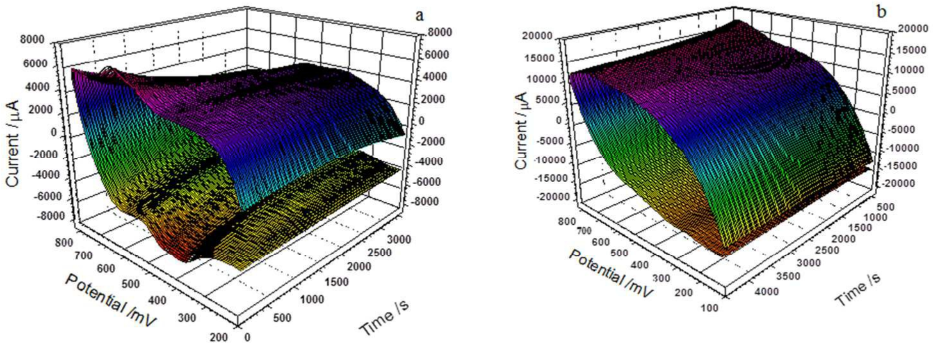

Fig. 7. 3D cyclic voltammogram of PANI (a) and PANI/NsMnO$_2$ (b) electrodes as a function of time by the scan rate of 50 mV s^{-1} in 1M H$_2$SO$_4$ solution (just 4000s showed).

FFTCCV technique could be considered as the best tool for examination the changes in the CVs and charge storage of a capacitor during the time. furthermore by using this technique one can study the behavior of electrochemical system momentarily. The CVs of two electrodes investigated in this technique in over time. Fig. 7 shows the three-dimensional (3D) CV of PANI and PANI/NsMnO$_2$ electrodes that were performed as a function of time, at the scan rate of 50 mVs^{-1}. The change in electrochemical behavior of composite electrode can be observed in these 3D CVs in over time. As can be seen after 4000 seconds PANI electrode losses its symmetrical shape and the magnitude of charge (Q) that surrounded by CV plots decreased. This behavior also occurred for PANI/NsMnO$_2$ composite electrode but this composite electrode preserved its symmetrical shape much more than PANI electrode.

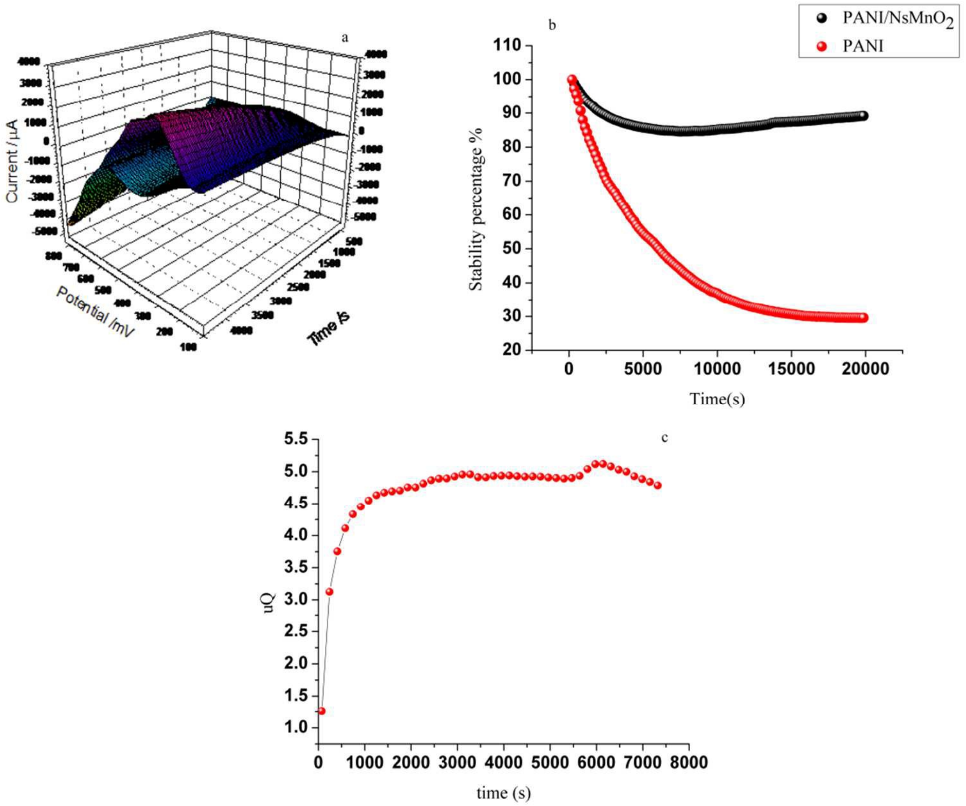

Fig. 8.3D differential voltametry of PANI/NsMnO$_2$ electrode measured at 50 mV s^{-1} for PANI/NsMnO$_2$ electrode (a) stability of two electrode after conseqtive cycles at 50 mV s^{-1} for 20000 s (b) differnce between capacitive current of the charge and discharge curves separately as a function of time at 50 mV s^{-1}for PANI/NsMnO$_2$(c).

Fig 8. presents some results that obtained by FFTCCV technique for PANI/NsMnO$_2$ composite electrode for consecutive CVs. Fig 8a) shows the 3D differential voltametry of PANI/NsMnO$_2$ electrode measured at 50 mV s^{-1} for PANI/NsMnO$_2$ electrode. In fact, the details of the occurring changes can even be seen well, when the current at recorded CVs subtracted from the current at reference voltammogram, where the reference voltammogram is obtained by averaging 5 FFTCCV voltammogram in the beginning of the measurement. The absolute capacitive charge changes (ΔQ_n) calculation for this operation is as follows equation:

$$\Delta Q_n = \int_{E_1}^{E_2} \Delta i_{(n,E)} dE - ave\left[\int_{E_1}^{E_2} \Delta i_{(m,E)} dE\right] \text{For n>0} \quad (4)$$

Or

$$\Delta Q_n = Q_n - Q_{ave} \quad (5)$$

Where Q_{ave} and Q_n are the calculated average charges at the selected potential range, E_1 to E_2, from m cyclic voltammograms and the calculated charge at the same potential range from subsequent n^{th} cyclic voltammogram, respectively. The computer program algorithm for calculating the detector response was:

$$\Delta Q(n\tau) = \frac{\Delta E}{\nu}\left(\sum_{E=E1}^{E=E2} i_{(n,E)} - \sum_{E=E1}^{E=E2} i_{(n_r,E)}\right) \quad (6)$$

In this equation, t is the time period between subsequent scans, v is the scan rate, ΔE is the potential difference between two subsequent points on the cyclic voltammogram, $i_{(n,\ E)}$ represents at the recorded cyclic voltammogram during the n^{th} scan and $i_{(nr,\ E)}$ is the reference current at stored cyclic voltammogram in the computer memory. The reference cyclic voltammogram was obtained by averaging a few recorded cyclic voltammograms at the beginning experiment. As can be seen in the Fig 8a) there are two peak in the potential range of 0.4 to 0.6V,that related to the oxidation of PANI, which have be seen in the CVs.[9] As shown in this figure there is a deceleration of current in the high positive potential range. this deceleration shows that the changes in oxidative state are more than reductive one. Fig 8b) shows the electrochemical stability of PANI and PANI/NsMnO$_2$ electrodes that examined in 1M H_2SO_4 solution by FFTCCV technique after continuous cycles for 20000 seconds with the scan rate of 50 mV s^{-1}. After sequence cycles because of degradation of conductive polymers, the stability of polymer electrode decreased.[10] As can be seen PANI/NsMnO_2 composite electrode has more stability than PANI electrode, whereas after 20000 seconds PANI electrode just has 30% of its capacitance related to first cycle, the PANI/NsMnO_2 composite electrode loss just 10% of its capacitance and preserved stable. Fig 8c shows the difference between the charge and discharge curves of PANI/NsMnO_2 composite electrode. By increasing the time and therefore the number of cycles, differences between charge and discharge currents got bigger and then after 1000 s reach to a constant number. This increasing of difference related to insertion and deinsertion of doping ions, in which a few number of ions after interance to the polymer film trapped to the polymer network and can't exit. Reaching to a constant number shows that those porosity in the polymer film which trap the ions were filled and then the columbic efficiency of electrode be compelete. With using FFTCCV technique one can following the change of CVs, cycle by cycle for study the capacitive behavior of composite electrode. This data processing operation was carried out simultaneously with data acquisition during experiments.

4 Conclusion

In this paper the application of a composite from $NsMnO_2$ and PANI was studied that allows to form a three dimensional volumetric supercapacitor with a quick charge propagation. The electrochemical method for synthesis of the composite let to a good capacitance results (507 F/g) compare to PANI (190 F/g). Uniform distribution of $NsMnO_2$ with the average size of 60nm achieved. Presence of $NsMnO_2$ cause to increasing the capacitance of composite electrode, furthermore PANI/$NsMnO_2$ composites shows a better cyclability than PANI electrode with a moderate loss of capacitance values (10% for composite electrode). EIS, CV and CD studies are in agreement together. The results obtained from the FFTCCV technique are very useful for investigation the electrochemical behavior of a single electrode as supercapacitor. Study the stability of electrodes, Columbic efficiency, 3D CVs for study the behavior change of composite electrode are some advantages of using this technique for study the supercapacitors.

ACKNOWLEDGEMENT

The authors are grateful to the Research Council of University of Tehran for the financial support of this work.

References

1. B. E, Conway**,** Electrochemical Supercapacitors: Scientific Fundamentals and Technological Application, Scientific Fun**.** New York : Kluwer Academic/Plenum Publishers, 1999. p. 18.
2. R. Kötz, M. Carlen**,** *Electrochim. Acta*, 2000, 45, 2483-2498.
3. S. Devaraj, N. Munichandraiah, *J. Phys. Chem. C*, 2008, 112, 4406-4417.
4. A. Ehsani**,** *prog .org. coat*, 2015, 78, 133-139.
5. Hui Xia, Jinkui Feng, Hailong Wang, Man On Lai, Li Lu**,** *J. Power Sources*, 2010, 195, 4410-4413.
6. P.W. Ruch, L.J. Hardwick, M. Hahn, A. Foelske, R. Ko¨tz, A. Wokaun. *Carbon*, 2009, 47, 38-52 .
7. K. Jurewicz, S. Delpeux, V. Bertagna, F. B'eguin, E. Frackowiak**,** *Chem. P. Lett*, 2001, 347, 36-40.
8. Khomenko, E. Frackowiak, F. Beguin**,** *Electrochim Acta*, 2005, 50, 2499-2506.
9. Hairui Zhang, Jixiao Wang, Yinying Chen, Zhi Wang, Shichang Wang, *Electrochim Acta*, 2013, 105, 69-74.
10. K. Lota, V. Khomenko, E. Frackowiak**,** *J. Phy & Chem. Solids*, 65, 2004, 295-301.
11. L.D. Arsov, W. Plieth, G. Koûmehl**,** *J. Solid State Electrochem*, 2, 1998, 355-361.
12. E. Frackowiak, V. Khomenko, K. Jurewicz, K. Lota, F. B´eguin**,** *J. Power Sources*, 2006, 153**,** 413–418.
13. Ye Hou, Yingwen Cheng, T. Hobson, Jie Liu**,** *Nano Lett*, 2010, 10 , 2727–2733.
14. Hualan Wang, Qingli Hao, Xujie Yang, Lude Lu, Xin Wang**,** *ACS Appl Mater Interfaces*, 2010, 2, 821-828.
15. Peng Lv, Yi Y. Feng, Yu Li, Wei Feng, *J. Power Sources*, 2012, 220. 160-168.
16. Pan Xiong, Huajie Huang, Xin Wang**,** *J. Power Sources*. 2014, 245, 937-946.

17. Shinichiro Oke, Masanobu Yamamoto, Kenji Shinohara, Hirofumi Takikawa, *Chem. Eng. J*, 2009, 146, 434–438 .
18. Xin-hui Yang, Yong-gangWang, Huan-ming Xiong, Yong-yao Xi, *Electrochim Acta*, 2007, 53, 752–757.
19. Yan-jing Yang, En-Hui Liu, Li-min Li, Zheng-zheng Huang, Hai-jie Shen, Xiao-xia Xiang**,** *J. Alloys. Compounds*, 2009, 487, 564–567.
20. En-Hui Liu, Xiang-Yun Meng , Rui Ding , Ji-Cheng Zhou , Song-Ting Tan**,** *Mat. Lett*, 2007, 61, 3486–3489.
21. V. Subramanian, Hongwei Zhu, BingqingWei**,** *J. Power Sources*, 2006, 159, 361–364.
22. Alireza Zolfaghari, Fatemeh Ataherian, Mehdi Ghaemi, Ameneh Gholami, *Electrochim Acta*, 2007, 52, 2806–2814.
23. N. Plesu, A. Kellenberger, M. Mihali, N. Vaszilcsin, *j. non-cryst. Solids*, 2010, 356, 1081-1088.
24. M.R. Ganjali, P. Norouzi, M. Ghorbani, A. Sepehri, *Talanta*, 2005, 66, 1225-1233.
25. P. Norouzi, M. Pirali-Hamedani, F. Faridbod, M. R. Ganjali**,** *Int. J. Electrochem. Sci,* 2010, 5, 1225 - 1235.
26. M. Sedaghat, P. Norouzi, J. Shamsi**,** *Anal. Bioanal. Electrochem*, 2014, 6, 43-53.
27. P. Norouzi, B. Larijani, M. R. Ganjali, F. Faridbod**,** *Int. J. Electrochem. Sci,* 2012, 7, 10414 - 10426.
28. P. Daneshgar, P. Norouzi , M. R.Ganjali, *Sensor Actuator **b**-chem*, 2009, 136, 66-72.
29. A. Ehsani, S. Adeli, F. Babaei, H. Mostaanzadeh, M. Nasrollahzadeh, *J. Electroanal. Chem*, 2014, 713, 91–97.
30. A. Ehsani, M. G. Mahjani, M. Jafarian, A. Naeemy, *Electrochim. Acta*, 2012, 71, 128-133.
31. A.H. Gemeay, I.A. Mansour, R.G. El-Sharkawy, A.B. Zaki, *J. Eur. Polym*, 2005, 41, 2575-2583.
32. Y. Li, J. Gong, G. He, Y. Deng, S, *Synth. Met*, 2011, 161, 56–61.

33. Z. Niu, Z. Yang, Z. Hu, Y. Lu, C.C. Han, *Adv Funct. Mater*, 2003, 13, 949-954.
34. Xiong Zhang, Liyan Ji, Shichao Zhang, Wensheng Yang, *J. Power Sources*, 2007, 173, 1017–1023 .
35. R.K. Sharma, L. Zhai, *Electrochim. Acta*, 2009, 54, 7148-7155.
36. A. Ehsani, M. Nasrollahzadeh, MG. Mahjani, R. Moshrefi, H. Mostaanzadeh, *Ind. Eng. Chem*, 2014, 20, 4363-4370.
37. A. Ehsani, M. G. Mahjani, R. Moshrefi, H. Mostaanzadeh, J. Shabani Shayeh, *RSC. Adv.* 2014, 4, 20031-20037.
38. A. Ehsani, MG. Mahjani, M. Bordbar, S. Adeli, J. *Electroanal. Chem*, 2013, 710, 29-35.